Electronic Supplementary Material

In-situ growth of phosphorized ZIF-67-derived amorphous CoP/Cu_2O@CF electrocatalyst for efficient hydrogen evolution reaction

Ruiwen Qi, Xiao Liu, Hongkai Bu, Xueqing Niu, Xiaoyang Ji, Junwei Ma (✉), Hongtao Gao (✉)

Key Laboratory of Optic-Electric Sensing and Analytical Chemistry for Life Sciences, MOE, College of Chemistry and Molecular Engineering, Qingdao University of Science and Technology, Qingdao 266042, China

E-mails: gaohtao@qust.edu.cn (Gao H); majw15@lzu.edu.cn (Ma J)

Theoretical Calculations

All DFT calculations are implemented using the Vienna ab initio Simulation Package (VASP) [1-3]. The electronic exchange and correlation are represented by the generalized gradient-corrected Perdew−Burke−Ernzerhof functional method (GGA-PBE) [4,5]. A plane-wave cutoff energy of 400 eV was used for the electronic wave function in all computations. The Brillouin zone was sampled by (2×2×1) and (4×4×1) Monkhorst-Pack k-point mesh for geometries relaxed and electronic structure calculations respectively [6]. In order to avoid the interaction between adjacent layers, a vacuum layer of 20 Å was established in the z-axis direction, and the force convergence criterion for structural optimization was set to 0.02 eV/Å. The dipole moment correction and the spin polarization setting were turned on. The van der Waals forces in the structure were considered and the correction was achieved using Grimme's DFT-D3 method [7]. The charge calculation was implemented using the Bader charge method developed by Henkelman and coworkers [8].

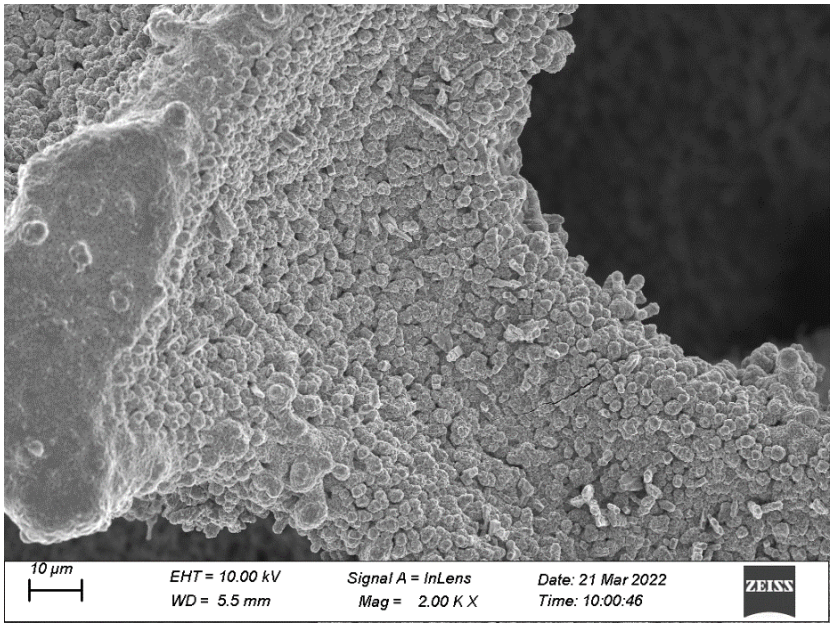

Fig.S1 Low magnification SEM images of CoP/Cu_2O@CF.

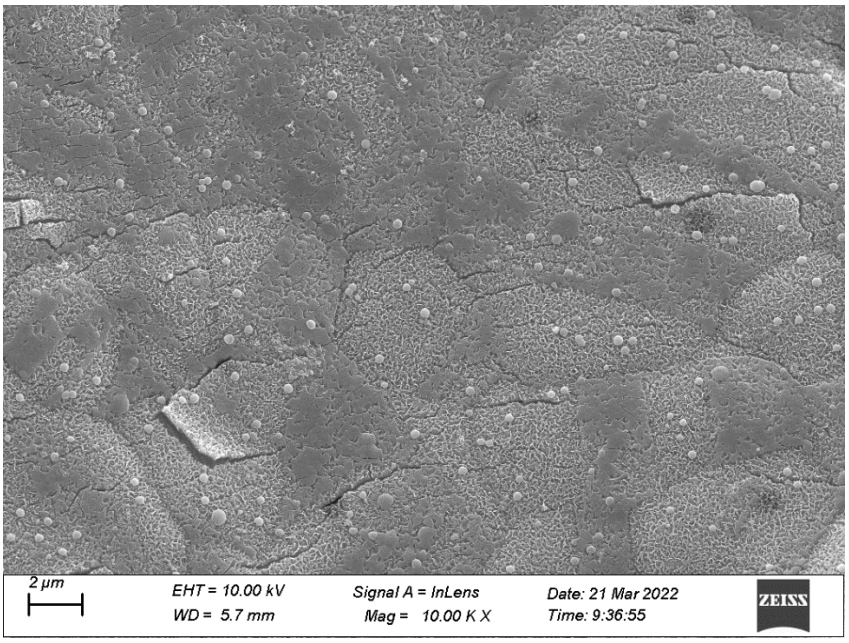

Fig.S2 SEM images of ZIF@CF.

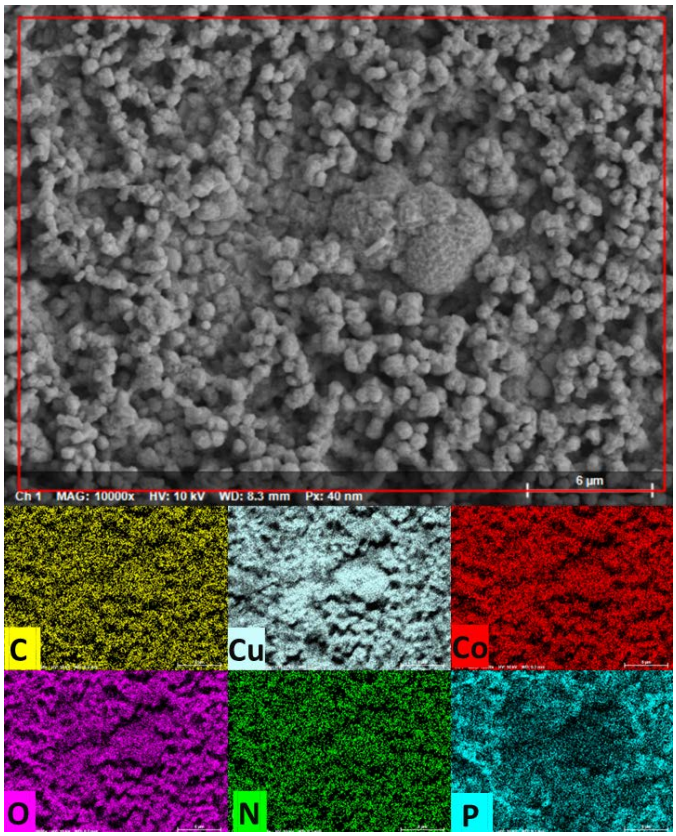

Fig.S3 elemental mapping images of CoP/Cu_2O@CF.

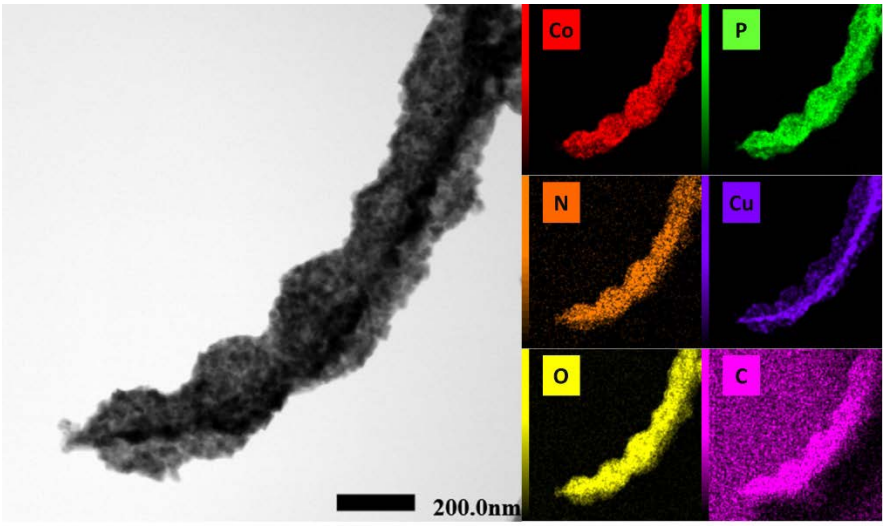

Fig.S4 TEM images and elemental mapping images of CoP/Cu_2O@CF.

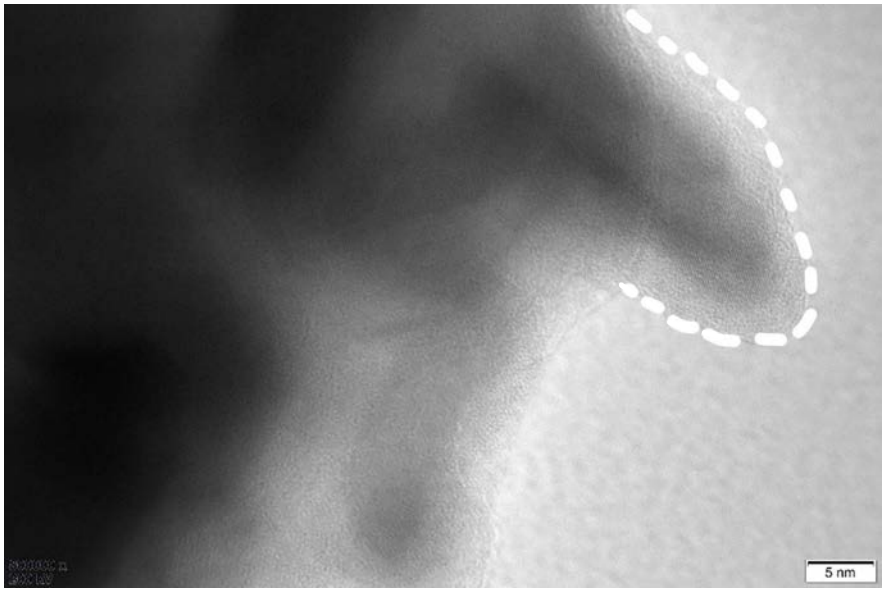

Fig.S5 HRTEM image of CoP/Cu_2O@CF.

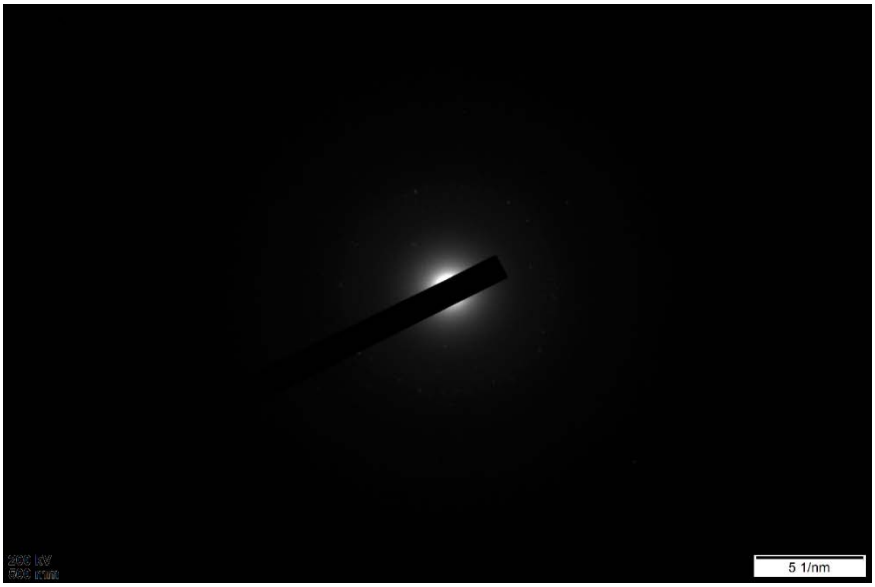

Fig.S6 SEAD pattern of CoP/Cu_2O@CF.

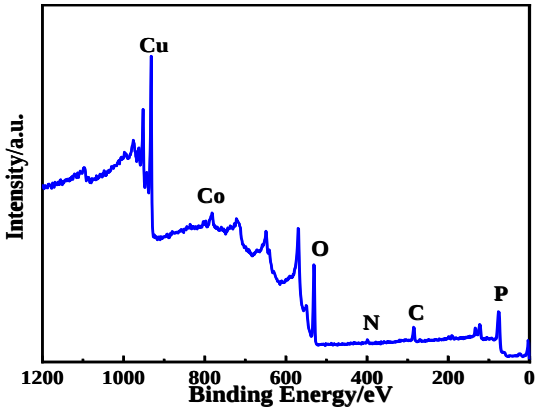

Fig.S7 Survey scan XPS plot of CoP/Cu_2O@CF.

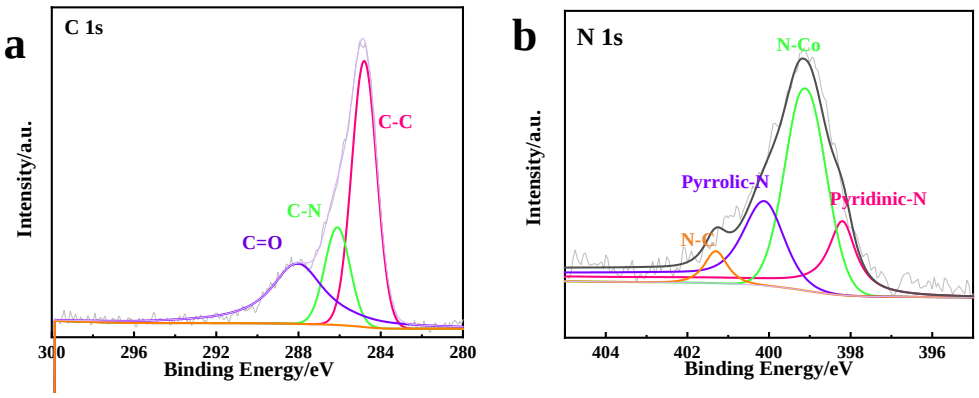

Fig.S8 CoP/Cu_2O@CF XPS Spectra of (a)C 1s, (b)N 1s.

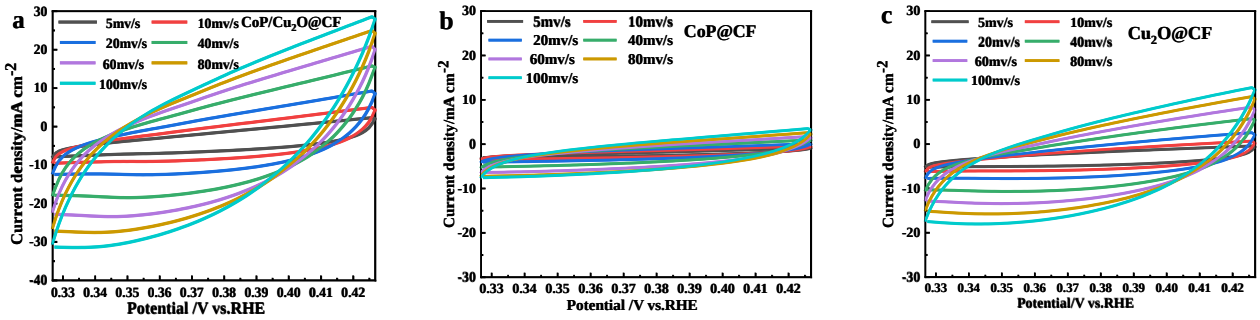

Fig.S9 CV curves of CoP/Cu_2O@CF, CoP@CF and Cu_2O@CF in the non-faradaic region at different scan rates.

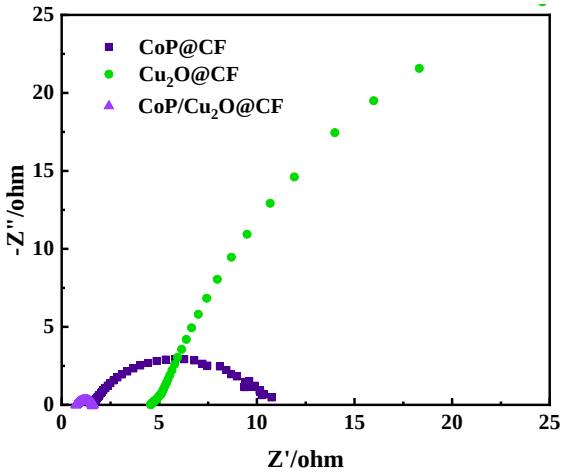

Fig.S10 Nyquist plots of the catalysts normalized by ECSA in 1 mol L^{-1} KOH solution.

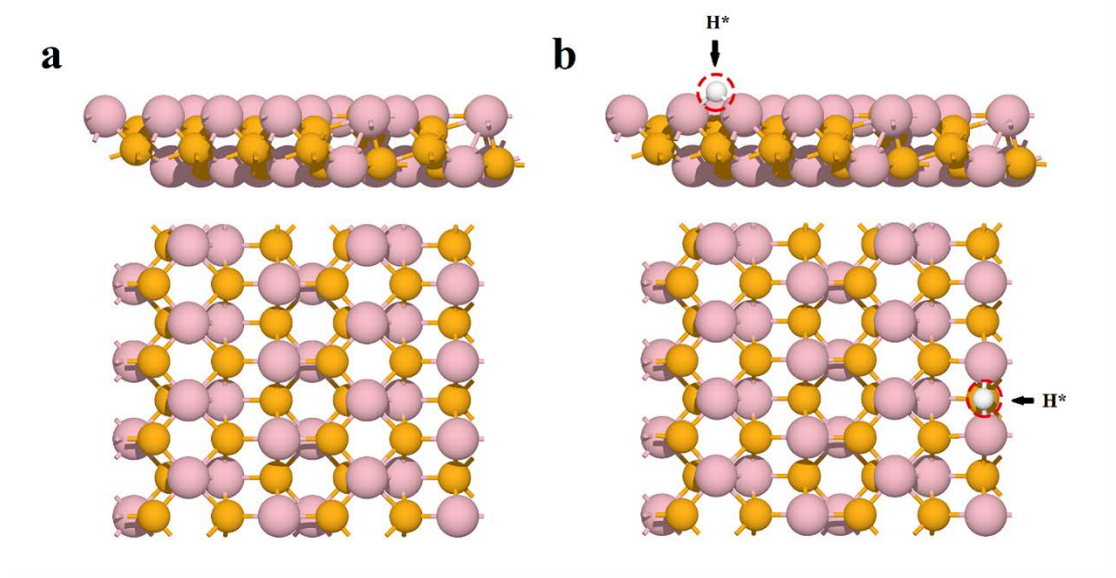

Fig.S11 Structure of cobalt phosphide (011) surface (a) and structure of hydrogen adsorption at the bridge site (b).

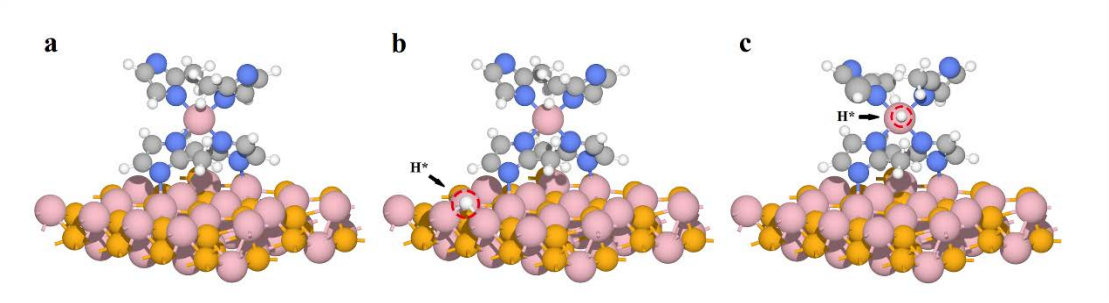

Fig.S12 Structure of CoP/ZIF before hydrogen adsorption (a), structure of hydrogen adsorbed at the bridge site of cobalt atoms (b), and adsorbed at cobalt atom in ZIF-67 (c).

Table S1 Correlation factor (R^2) of the linear plot of capacitive current vs. scan rate, double layer capacitance (C_{dl}), calculated ECSA of the prepared materials over CF, and the specific surface of the electrode estimated by multiplying the geometrical surface to ECSA ($A_{Elect.}=A_{Geom} \times ECSA$, $A_{Geom}=0.25\ cm^2$).

Materials	**R^2**	**C_{dl}/mF cm^{-2}**	**ECSA**	**A_{Elect}/cm^2**
CoP/Cu_2O@CF	0.94331	0.1572	3.93	0.9825
CoP@CF	0.98236	0.0892	2.23	0.5575
Cu_2O@CF	0.98129	0.0295	0.737	0.1843

References

1. Kresse G, Hafner J. Ab initio molecular-dynamics simulation of the liquid-metal-amorphous-semiconductor transition in germanium. Physical Review B, 1994, 49(20): 14251-14269
2. Kresse G, Furthmüller J. Efficient iterative schemes for ab initio total-energy calculations using a plane-wave basis set. Physical Review B, 1996, 54(16): 11169-11186
3. Kresse G, Furthmüller J. Efficiency of ab-initio total energy calculations for metals and semiconductors using a plane-wave basis set. Computational Materials Science, 1996, 6(1): 15-50
4. Perdew J P, Burke K, Ernzerhof M. Generalized gradient approximation made simple. Physical Review Letters, 1996, 77(18): 3865-3868
5. Blöchl P E. Projector augmented-wave method. Physical Review B, 1994, 50(24): 17953-17979
6. Chadi D J. Special points for Brillouin-zone integrations. Physical Review B, 1977, 16(4): 1746-1747
7. Grimme S. Semiempirical GGA-type density functional constructed with a long-range dispersion correction. Journal of Computational Chemistry, 2006, 27(15): 1787-1799
8. Tang W, Sanville E, Henkelman G. A grid-based Bader analysis algorithm without lattice bias. Journal of Physics: Condensed Matter, 2009, 21(8): 084204